Eur. Phys. J. B **80**, 223–232 (2011)
DOI: 10.1140/epjb/e2011-10756-3

THE EUROPEAN PHYSICAL JOURNAL B

Regular Article

A wavelet-based mode decomposition

S. Nicolay[a]

University of Liège, Department of Mathematics, 12, Grande Traverse Bât. B37, 4000 Liège, Belgium

Received 4 October 2010 / Received in final form 28 January 2011
Published online 9 March 2011 –

Abstract. We propose a wavelet-based method for analyzing non-stationary data. The idea, inspired by the empirical mode decomposition, is to decompose a data set into a finite number of components, well separated in the time-frequency plane, plus a residue, such that each component has a zero mean and is associated to one frequency only. When applied to climatic data, this method gives interesting results.

1 Introduction

The Fourier spectral analysis (see e.g. [1–3]) provides a simple yet powerful method for examining signals from a frequency point of view. It has been so much used that it has led to some abuses, especially when applied to non-linear or non-stationary signals. Indeed, this method seemed to be the only valid approach until the (re)discovering of the wavelets by Morlet in the eighties (see [4,5]). Since then, other fruitful frequency-based methods have been developed, one of them being the empirical mode decomposition (see [6]).

Here, we present a wavelet-based method that leads to the decomposition of a signal into zero mean components, each one being associated to a mean frequency. Unlike the Fourier transform, the proposed decomposition does not lead to pure cosines: a component is not identified with a fixed amplitude or frequency, they (slowly) evolve through time. As we will see, this allows to drastically decrease the number of modes associated to a function (compared to the Fourier transform). It is well known that most of the wavelet-based methods can not separate frequencies very well; however, in our case, we use this fact as an advantage: it is not always physically relevant to separate close tones, especially when dealing with non-stationary signals (see e.g. [7]). In some sense, the method proposed here amalgamates tones with close frequencies in a fully data-driven way.

This paper is organized as follows. We first give the basic definitions of the wavelet transform and introduce a family of wavelets, starting from the Morlet wavelet. We then present the scale spectrum, which allows to associate frequencies to a signal. This spectrum can be used to define a method that decomposes a signal into fundamental components. Each such component is associated to one frequency only.

The next section is devoted to the application of this method to "toy examples". We successively consider a signal defined by a sum of cosines, a cosine plus a noise and a cosine with a "shifting frequency".

In the final section, we consider the air temperature time series obtained from a weather station. The wavelet approach leads to the detection of three uncommon periods.

This method should prove well adapted for non-stationary signals and data with uncertain time scales, like paleoclimatic time series.

[a] e-mail: S.Nicolay@ulg.ac.be

2 Definitions

The aim of this section is to introduce a wavelet-based mode decomposition, leaning on a family of wavelets $\psi_{\alpha,\beta}$. Each mode is associated to one frequency, which can slowly evolve through time; no condition is imposed on the modulus.

2.1 The continuous wavelet transform

We briefly introduce the one-dimensional continuous wavelet transform of a function.

Let us first give the mathematical definition (for more details, see e.g. [8–10]). A wavelet (or mother wavelet) is a function ψ belonging to the space $L^1(\mathbb{R}) \cap L^2(\mathbb{R})$ that satisfies the admissibility condition

$$\int \frac{|\mathcal{F}\psi(\omega)|^2}{|\omega|}\, d\omega < \infty,$$

where $\mathcal{F}\psi$ denotes the Fourier transform of ψ. For such a condition to be satisfied, the equality $\mathcal{F}\psi(0) = 0$ has to hold (let us remark that this condition is not sufficient). In other words, the first moment of ψ vanishes, which explains the denomination "wavelet". The (one-dimensional) continuous wavelet transform (CWT) associated to ψ is

the operator defined as follows,

$$W : L^2(\mathbb{R}) \to L^2\left(\mathbb{R} \times \mathbb{R}_*^+; dt\frac{da}{a}\right)$$
$$f \mapsto \int f(x)\bar{\psi}\left(\frac{x-t}{a}\right)\frac{dx}{a},$$

where $\bar{\psi}$ denotes the complex conjugate of ψ; $Wf(t,a)$ is the wavelet transform of f at scale a and position t. The admissibility condition ensures that the function f can be recovered back from its CWT (for more details, see e.g. [8–10]).

The CWT was first introduced for analyzing seismic data and acoustic signals ([4,5]). It can be regarded as a mathematical microscope, for which position and magnification correspond to t and $1/a$ respectively, the performance of the optic being determined by the mother wavelet (see [11]). This tool has been successfully put into practice on numerous theoretical and applied problems (see e.g. [9,12,13]).

2.2 A new family of wavelets

We define here a family of wavelets depending on two parameters, starting from the celebrated Morlet wavelet. The first parameter allows to design wavelets that possess exactly n vanishing moments, while the second parameter is related to the localization (in frequency) of the wavelet.

The Morlet wavelet ψ_M is the function whose Fourier transform is

$$\mathcal{F}\psi_M(\omega) = \exp\left(-\frac{(\omega-\Omega)^2}{2}\right) - \exp\left(-\frac{\omega^2}{2}\right)\exp\left(-\frac{\Omega^2}{2}\right),$$

where Ω is a constant, called the central frequency of the wavelet. One usually chooses Ω larger than 5 (in one over time units), so that the second term in the previous inequality can be neglected to obtain $\mathcal{F}\psi_M(\omega) = \exp(-(\omega-\Omega)^2/2)$. Moreover, if $\Omega \geq 5$, the Morlet wavelet (both the exact and the approximate forms) satisfies $|\mathcal{F}\psi_M(\omega)| < 10^{-5}$ if $\omega \leq 0$; therefore, it is generally considered as a progressive wavelet (a wavelet ψ is progressive if $\omega \leq 0$ implies $\mathcal{F}\psi(\omega) = 0$, see e.g. [10]).

It is easy to check that the Morlet wavelet has exactly one vanishing moment (the approximated Morlet wavelet has no vanishing moment and is thus not really a wavelet, but an approximation of a wavelet). Let $\alpha, \beta > 0$ and define the function $\psi_{\alpha,\beta}$ through its Fourier transform as follows,

$$\mathcal{F}\psi_{\alpha,\beta}(\omega) = \sin\left(\frac{\pi\omega}{2\Omega}\right)^{\alpha}\exp\left(-\frac{(\omega-\Omega)^{\beta}}{2}\right).$$

This relation implies that $\psi_{\alpha,\beta}$ has exactly $[\alpha]$ vanishing moments (where $[\cdot]$ denotes the floor function). If $\alpha \geq 1$, the extrema of $\mathcal{F}\psi_{\alpha,\beta}$ can be obtained owing to the equation

$$\alpha\pi\cos\left(\frac{\pi\omega}{2\Omega}\right) = \beta\Omega(\omega-\Omega)^{\beta-1}\sin\left(\frac{\pi\omega}{2\Omega}\right).$$

Moreover, if $\beta = 2$, the function $\psi_{\alpha,\beta}$ can be explicitly obtained (using integration by parts). For example, we have

$$\psi_{1,2}(x) = \frac{1}{2\sqrt{2\pi}}\exp(i\Omega x) \times \exp\left(-\frac{(2\Omega x+\pi)^2}{8\Omega^2}\right)\left(\exp\left(\frac{\pi x}{\Omega}\right)+1\right)$$

and

$$\psi_{2,2}(x) = \frac{1}{4\sqrt{2\pi}}\exp(i\Omega x)\exp\left(-\frac{(\Omega x+\pi)^2}{2\Omega^2}\right) \times \left(\exp\left(\frac{2\pi x}{\Omega}\right)+\exp\left(\frac{\pi(2\Omega x+\pi)}{2\Omega^2}\right)+1\right).$$

We therefore have obtained a family of wavelets $\{\psi_{\alpha,\beta}\}$ such that $\psi_{\alpha,\beta}$ has exactly $[\alpha]$ vanishing moments and β controls the decay rate of the wavelet in the frequency space. Moreover, if the Morlet wavelet is supposed to be a progressive wavelet, so can be $\psi_{\alpha,\beta}$.

2.3 The scale spectrum

The scale spectrum is an alternative to the usual Fourier spectrum-based tools. It allows to deal with non-stationary signals if their properties "do not evolve too quickly" (in order to preserve a meaningful notion of frequency, see e.g. [2,14]). We recall here the definitions as well as the basic properties.

The scale spectrum is based on the following remark. If ψ is a progressive wavelet, we have

$$W[\cos(\omega_0 x)](t,a) = \frac{1}{2}\exp(i\omega_0 t)\overline{\mathcal{F}\psi}(a\omega_0).$$

If $\mathcal{F}\psi$ is a real function, the modulus of the CWT is given by $\mathcal{F}\psi(a\omega_0)$ and the phase by $\exp(i\omega_0 t)$. The a priori unknown (angular) frequency ω_0 can be obtained back from $\mathcal{F}\psi$: for example, if ψ is of the form $\psi_{\alpha,\beta}$ (the Morlet wavelet is the wavelet $\psi_{0,2}$), the maximum of $\mathcal{F}\psi_{\alpha,\beta}(a\omega_0)$ is reached for $a = \Omega/\omega_0$.

The (marginal) scale spectrum of a function f is

$$\Lambda(a) = M|Wf(\cdot,a)|,$$

where M denotes the mean over time. Let us remark that this spectrum is not defined in terms of density. Such a spectrum can be interpreted in a similar manner as the Fourier spectrum, allowing to study a function from a frequency point of view.

It is important to remark that the scale spectrum has a very different meaning from the Fourier spectrum. The existence of energy at a given frequency in the Fourier spectrum means that the corresponding cosine wave is one of the fundamental components of the signal; such a wave can thus be observed through the whole time span of the signal. The presence of energy at the same frequency in the scale spectrum only means that there is a higher likelihood for such a wave to have appeared locally. Unlike the

Fourier transform, the scale spectrum can thus be used to study non-stationary signals. Since the scale spectrum is not discrete, it may be unable to make the distinction between two close frequencies, but, on the other hand, it can deal with frequency drifts.

It can be shown that the scale spectrum is a rather efficient method to detect cycles in a signal, even if it is perturbed with a colored noise, or if it involves so-called "pseudo-frequencies" (see e.g. [15,16]).

2.4 A wavelet-based mode decomposition

The scale spectrum allows to decompose a function into building block functions with slowly varying amplitudes and frequencies. Such a decomposition is therefore fundamentally different from the Fourier series based methods, since here we do not deal with constant modulus and frequency.

Let f be a square-integrable real function and Λ be the associated scale spectrum; we will denote by $a_1, \ldots, a_J$ the abscissa where Λ reaches a maximum (in practice, we can suppose that J is a natural number). For $j \in \{1, \ldots, J\}$, let

$$f_j(x) = \cos\Big(\arg\big(Wf(x, a_j)\big)\Big)\,|Wf(x, a_j)|$$

and

$$f_0(x) = f(x) - \sum_{j=1}^{J} f_j(x).$$

By definition, one has $f = \sum_{j=0}^{J} f_j$. Moreover, if $j \geq 1$, f_j can be associated with a constant (angular) frequency ($\omega_j = \Omega/a_j$ if the wavelet is of the form $\psi_{\alpha,\beta}$), the phase being given by $\arg\big(Wf(x, a_j)\big)$. However, although f_j ($j \geq 1$) is associated to a frequency ω_j, it is not fixed in time, that is, we do not rigorously have

$$f_j(x) = |Wf(x, a_j)|\cos(\omega_j x + \phi),$$

for a constant ϕ. This adds additional flexibility to the decomposition.

Since the CWT transform associates a complex signal to a real signal, one could interpret (supposing that the following expression is meaningful) the derivative of $\arg(Wf(x, a_j))$ as the instantaneous (angular) frequency of f_j ($j \geq 1$), keeping in mind that one always has to be careful with such an explanation (see e.g. [17]).

Let us remark that if P is a polynomial of degree α and if the wavelet has at least $\alpha + 1$ vanishing moments, the components f_j ($j \geq 1$) of the function f are also the components of the function $f + P$, that is, the above decomposition is blind to lower degree polynomials. We will now show that it is an efficient tool when dealing with simple non-stationary signals.

3 Application to theoretical examples

In this section, we show that the decomposition proposed above leads to satisfactory results for simple signals. The wavelet chosen for these applications is $\psi_{1,2}$.

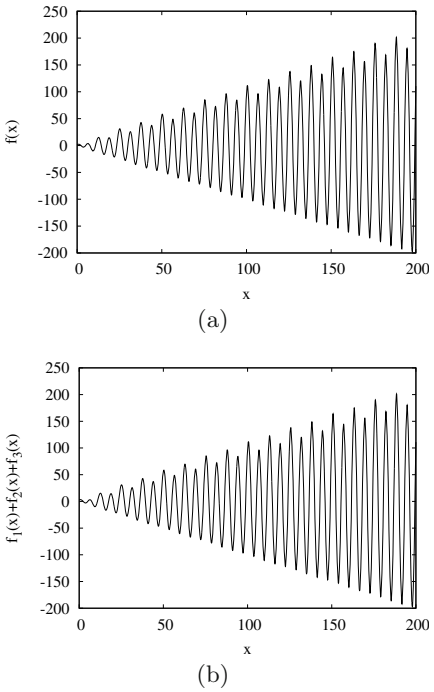

Fig. 1. The original signal $f(x) = x\cos(x) + \sqrt{x}\cos(x/2) + \cos(x/4)$ (a) and the reconstruction $f_1 + f_2 + f_3$ associated to f (b).

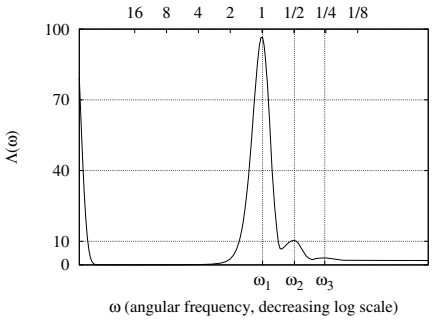

Fig. 2. The scale spectrum Λ of the function $f(x) = x\cos(x) + \sqrt{x}\cos(x/2) + \cos(x/4)$. The abscissa are in logarithmic scale.

3.1 Sum of cosines

The most basic test certainly consists in applying the above decomposition to a sum of cosines. We already know that a function $f(x) = \sum_{j=1}^{J}\cos(\omega_j x)$ will be associated to J components f_j of the form $f_j(x) = \cos(\omega_j x)$, provided that the (angular) frequencies ω_j are sufficiently different from each other, that is, $|\omega_j - \omega_{j+1}| > \varepsilon_j$ ($1 \leq j < J$), where ε_j depends on the chosen wavelet (see [15,16]). However, such a result can be obtained using other methods, such as the Fourier transform. We test here our methodology on functions made of waves with non-constant amplitudes.

Let $f(x) = x\cos(x) + \sqrt{|x|}\cos(x/2) + \cos(x/4)$ (see Fig. 1a). The scale spectrum associated to f displays three maxima corresponding to the (angular) frequencies $\omega_1 = 0.9916$, $\omega_2 = 0.4958$ and $\omega_3 = 0.2566$ respectively (see Fig. 2), which compare very well to the real values

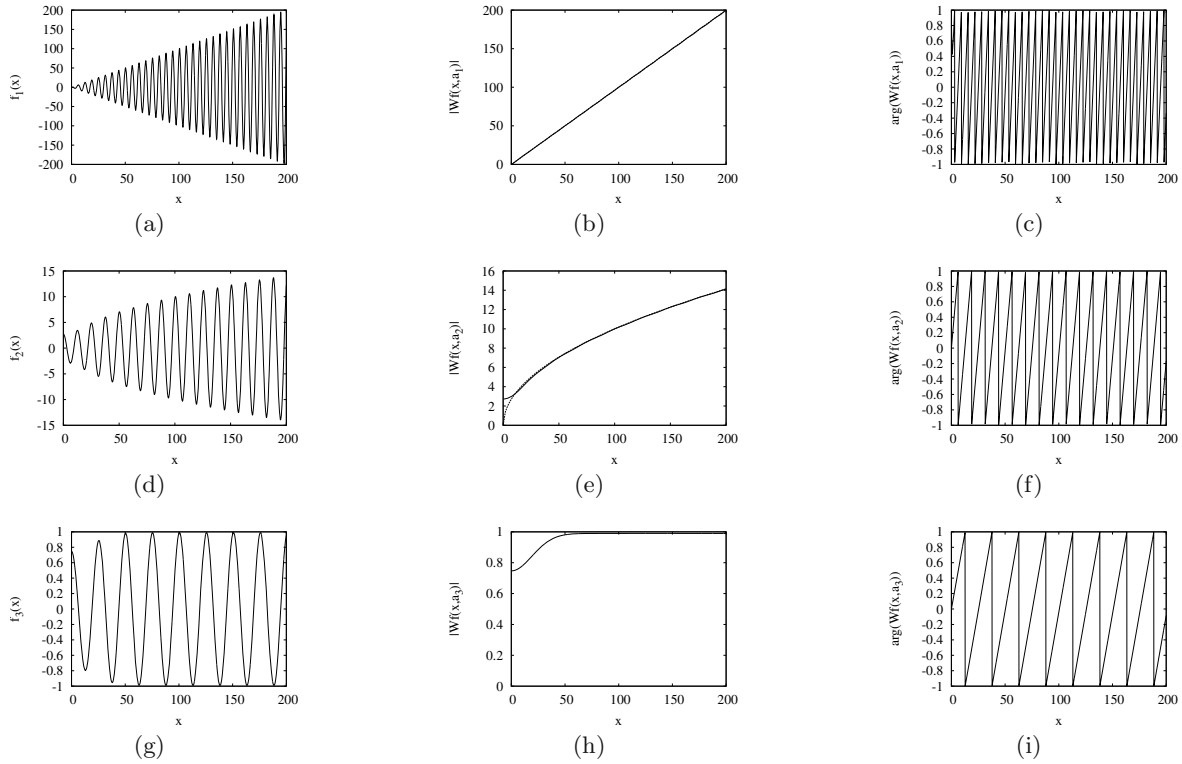

Fig. 3. The wavelet decomposition of $f = x\cos(x) + \sqrt{|x|}\cos(x/2) + \cos(x/4)$: the first (a), the second (d) and the third (g) component, as well as the modulus of the first (b), the second (e) and the third (h) component and the phase of the first (c), the second (f) and the third (i) component.

(which are 1, 0.5 and 0.25). Let us remark that the ordinates $\Lambda(\omega_1) = 96.505$, $\Lambda(\omega_2) = 10.336$ and $\Lambda(\omega_3) = 2.946$ give the mean amplitude associated to the (angular) frequencies ω_1, ω_2 and ω_3.

The wavelet decomposition thus leads to three components f_1, f_2, and f_3. As shown in Figure 1b, the signal $f_1 + f_2 + f_3$ is similar to f: the (Pearson) correlation between f and $f_1 + f_2 + f_3$ is greater than 0.998 and the root mean square error (RMSE) is smaller than 0.284. The components f_1, f_2 and f_3 as well as the associated modulus $|Wf(x, a_j)|$ and phase $\arg\big(Wf(x, a_j)\big)$ are represented in Figure 3. Here also, the numerical values are close to the real ones, excepted for the abscissa near the origin where the methodology do not manage to separate the moduli correctly (see Figs. 3e and 3h).

3.2 Cosine with noise

The behavior of the wavelet decomposition when applied to a noisy signal is of primary importance. If a Gaussian white noise is added to a cosine, the lowest scales will be mainly affected. Of course, the number of altered scales depends on the standard deviation of the noise. The results are similar if one replaces the white noise with a red noise, namely an autoregressive model of the first order or AR(1).

Let $f(x) = \cos(x) + Z(x)$, where Z is a Gaussian white noise with zero-mean and unit variance (see Fig. 4a). The scale spectrum of a realization of such a process f displays a typical decreasing shape. As an example, the realization shown in Figure 5 exhibits five maxima corresponding to the (angular) frequencies $\omega_1 = 27.62$, $\omega_2 = 0.996$, $\omega_3 = 0.108$, $\omega_4 = 0.049$ and $\omega_5 = 0.031$ respectively. We performed 1000 such realizations and the number of maxima always varied between 3 and 6. However, one directly sees in Figure 5 that the three last frequencies can be neglected when compared to ω_1 and ω_2. More rigorously, the variance associated to the components 3, 4 and 5 are $V_3 = 1.14 \times 10^{-3}$, $V_4 = 4.63 \times 10^{-4}$ and $V_5 = 4.55 \times 10^{-4}$ respectively, so that their contribution may be judged unsignificant, since the variance of the two first components are $V_1 = 4.44 \times 10^{-1}$ and $V_2 = 4.9 \times 10^{-1}$ respectively. As shown in Figure 6, the scale spectrum of f can indeed be decomposed into two scale spectra. The first one, associated to $\cos(x)$, displays one maximum associated to the (angular) frequency 0.996. The second one, associated to Z, features the decreasing profile observed in Figure 5 and displays several maxima, but only the first one, corresponding to the (angular) frequency 27.62 can be judged as significant. This is the only maximum that is observed in each realization of Z: as shown in Figure 6b, the shape of the spectrum associated to each realization of Z is characteristic.

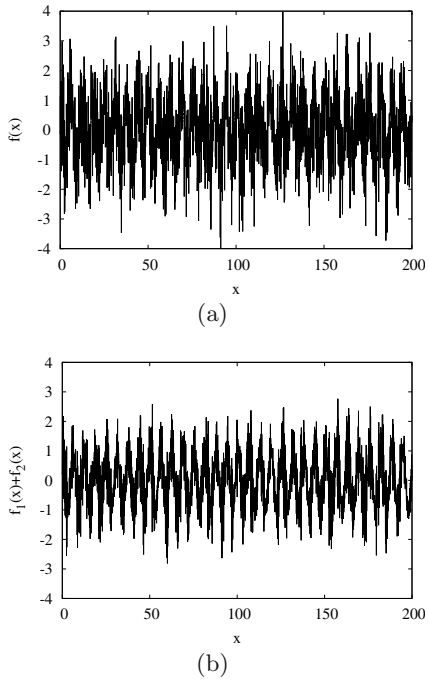

Fig. 4. A realization of the process $f = \cos + Z$, where Z is a Gaussian white noise (a) and the reconstruction $f_1 + f_2$ associated to f (b).

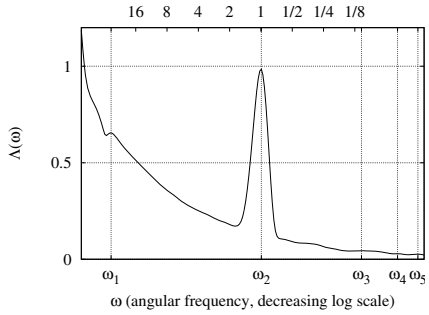

Fig. 5. The scale spectrum Λ of a realization of $f(x) = \cos(x) + Z(x)$. The abscissa are in logarithmic scale.

The two first components of the realization f_1 and f_2 associated to ω_1 and ω_2 respectively are shown in Figure 7. Let us remark that the amplitude of the second component, corresponding to cos, can not be considered as a constant. However the correlation between f and f_2 is equal to 0.577, while the correlation between f and cos is equal to 0.566, which is corroborated by the RMSE, since we get 1.005 and 1.013 respectively. Therefore, the decomposition $f_1 + f_2$ proposed by the wavelet spectrum is, in some way, a better decomposition than the decomposition consisting in a random noise plus cos. The correlation between f and $f_1 + f_2$ is equal to 0.758 ± 10^{-3} and the RMSE is equal to 0.8 ± 10^{-3}.

If the Gaussian white noise Z is replaced by an AR(1) model, that is, if Z now satisfies

$$Z(n+1) = \alpha Z(n) + \eta(n),$$

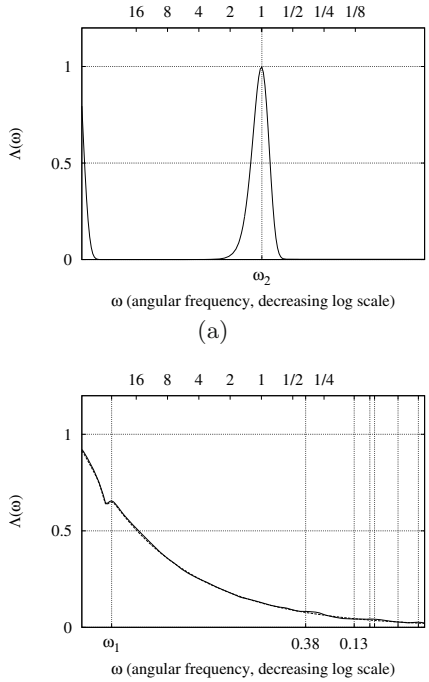

Fig. 6. The scale spectra Λ of the function $f(x) = \cos(x)$ (a) and a realization of a Gaussian noise Z (solid lines) superimposed to a mean spectrum of a Gaussian noise (1000 realizations, dashed lines) (b). The abscissa are in logarithmic scale.

with $0 < \alpha < 1$, where η is a Gaussian white noise with zero mean and unit variance (see e.g. [18]; let us remark that the mean and the variance associated to Z are respectively 0 and $(1-\alpha^2)^{-1}$), the result are similar. As shown in Figure 8, the shape of the scale spectrum of such a process is also a typical one and each realization is very close to the mean profile. Further theoretical investigations should be carried out to explain how the models Z used above induce the characteristic profiles observed in Figures 6b and 8.

In conclusion, if a pure cosine function is perturbed by a Gaussian white noise or an AR(1) model, additional components will be associated to the signal. They are of two types: components with low frequencies and low amplitude and a component with a higher frequency. Components of the first type are associated to a specific realization and do not perturb the signal too much, since they can be considered as negligible. Components of the second type can be non-negligible if the variance of the noise is too large.

3.3 Cosine with a shifting frequency

The main advantage of the wavelet decomposition is its ability to detect pseudo-frequencies, that is, to associate a mode with a "time-varying frequency" (this denomination will be made clearer in the following paragraph).

Let $f(x) = \cos(\omega(x)x)$, with $\omega(x) = (1+\ln(|x|)/50)/4$; this function, as well as the function cos are represented in

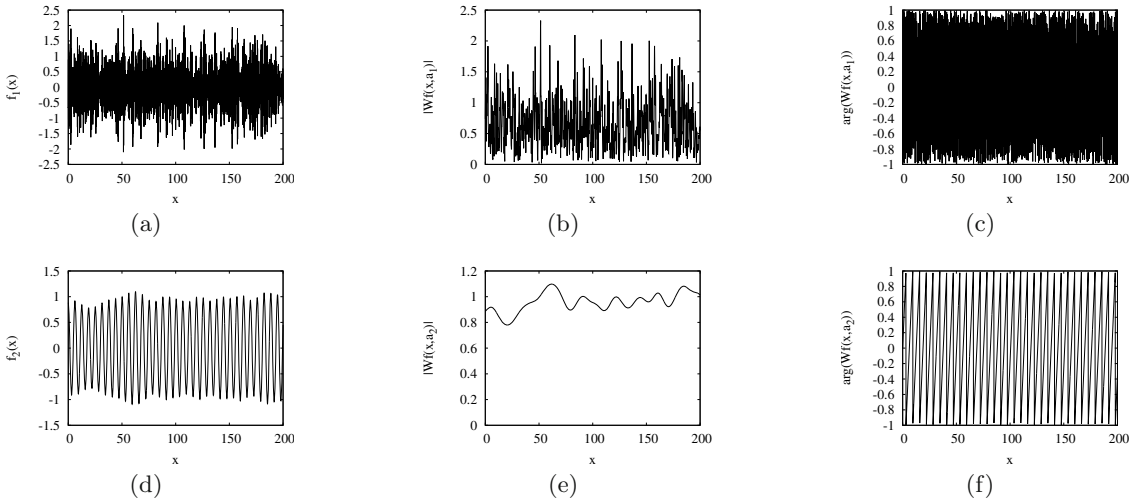

Fig. 7. The wavelet decomposition of $f = \cos + Z$, where Z is a Gaussian white noise: the first (a) and the second (d) component, as well as the modulus of the first (b) and the second (e) component and the phase of the first (c) and the second (f) component.

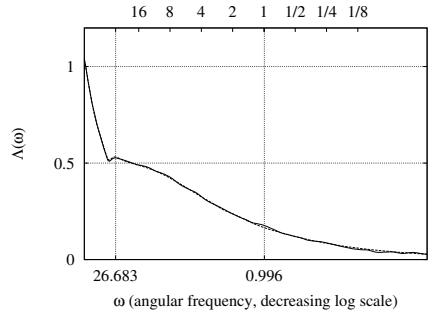

Fig. 8. The scale spectrum Λ of a realization of an AR(1) model Z with $\alpha = 0.25$ (solid lines) superimposed to a mean spectrum of the same AR(1) model (1000 realizations, dashed lines).

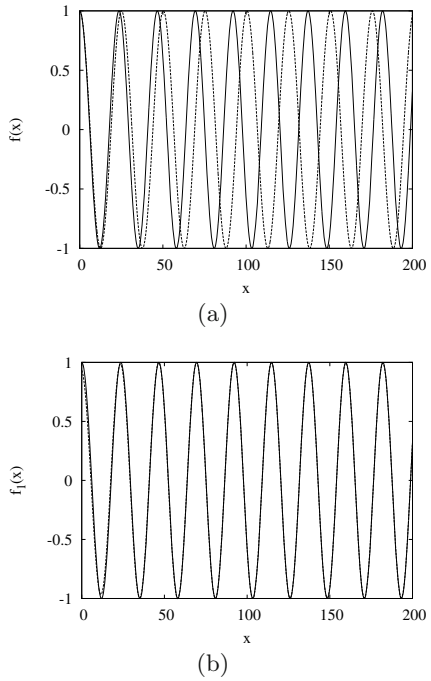

Fig. 9. The function $f(x) = \cos(\omega(x)x)$ (solid line) superimposed to the function $\cos(x/4)$ (dashed lines) (a) and the reconstruction f_1 (solid lines) associated to f superimposed to f (dashed lines) (b).

Figure 9a. The scale spectrum of f displays one maximum corresponding to the (angular) frequency $\omega_1 = 0.256$ (see Fig. 10; the scale spectrum of the function $\cos(x/4)$ is also represented in dashed lines).

The wavelet decomposition of f thus leads to only one mode f_1 (see Fig. 11), which remarkably matches the original signal, as shown in Figure 9b, although the modulus near the origin is underestimated (see Fig. 11b). The correlation between f and f_1 is larger than 0.995 and the RMSE is smaller than 0.03.

4 Application to temperature time series

As an application, we will apply the scale spectrum-based decomposition to the near-surface air temperature time series of the Verhojansk (Respublika Sakha (Yakutiya), Russian Federation, 67.5°N, 133.4°E) weather station (in Celsius degrees, monthly sampled data) collected from the GISS data sets (see [19]). This station has been chosen because such an area displays a continental climate, where the influence of the sun is highly prevailing (following [20], the climate classification of Verhojansk is EC).

4.1 Decomposition

The near-surface air temperature of the Verhojansk weather station are represented in Figure 12a. The scale spectrum of this time series displays four maxima corresponding to (approximatively) 4, 12, 30

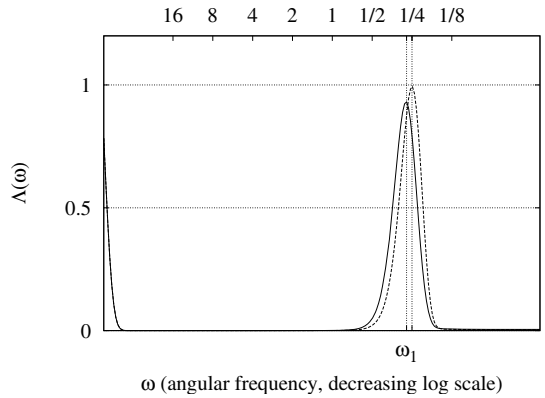

Fig. 10. The scale spectra Λ of the functions $f(x) = \cos(\omega(x)x)$ (solid lines) and $f(x) = \cos(x/4)$ (dashed lines). The abscissa are in logarithmic scale.

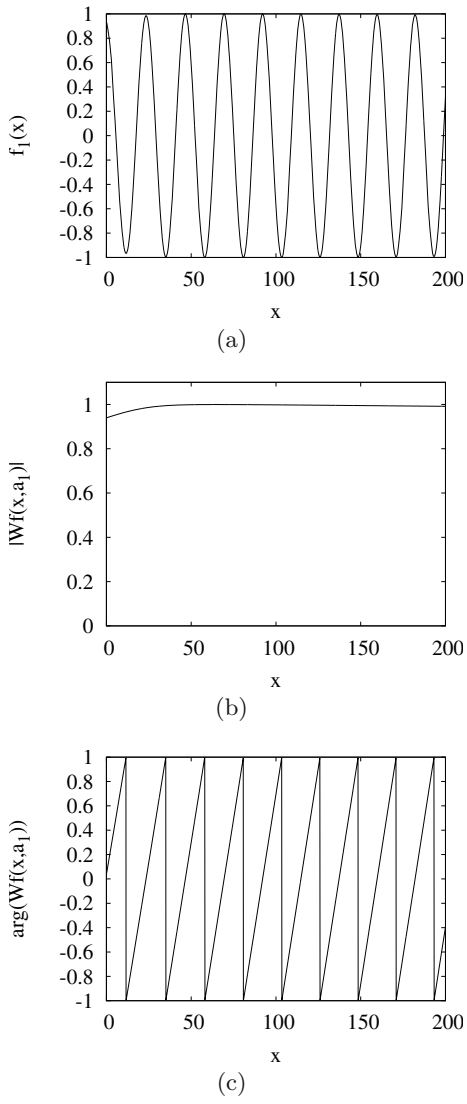

Fig. 11. The wavelet decomposition of $f(x) = \cos(\omega(x)x)$: the component (a), as well as the modulus (b) and the phase (c) of the component.

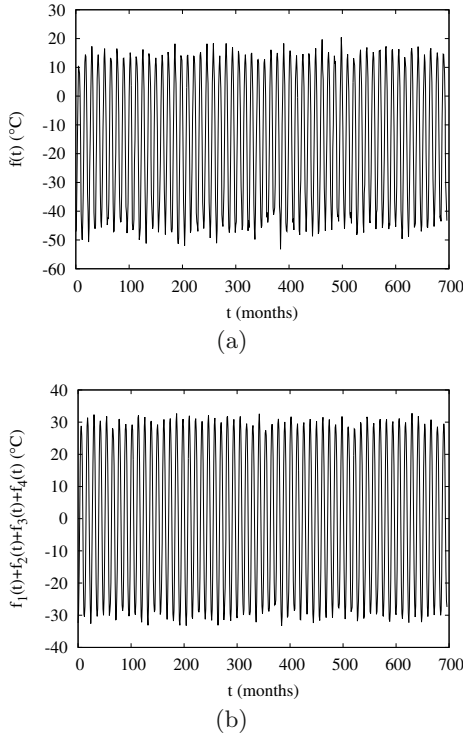

Fig. 12. The near-surface air temperature records from Verhojansk (a) and the associated reconstruction $f_1 + f_2 + f_3 + f_4$ (b).

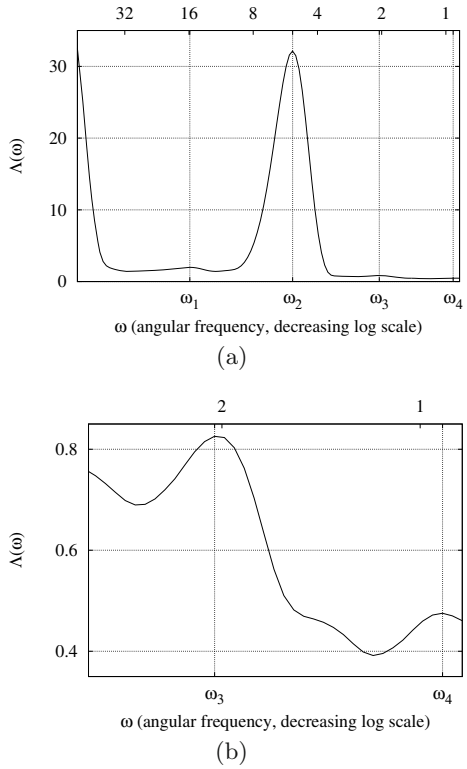

Fig. 13. The scale spectrum Λ of the temperature records from Verhojansk: the whole spectrum (a) and the end of the spectrum (b). The abscissa are in logarithmic scale.

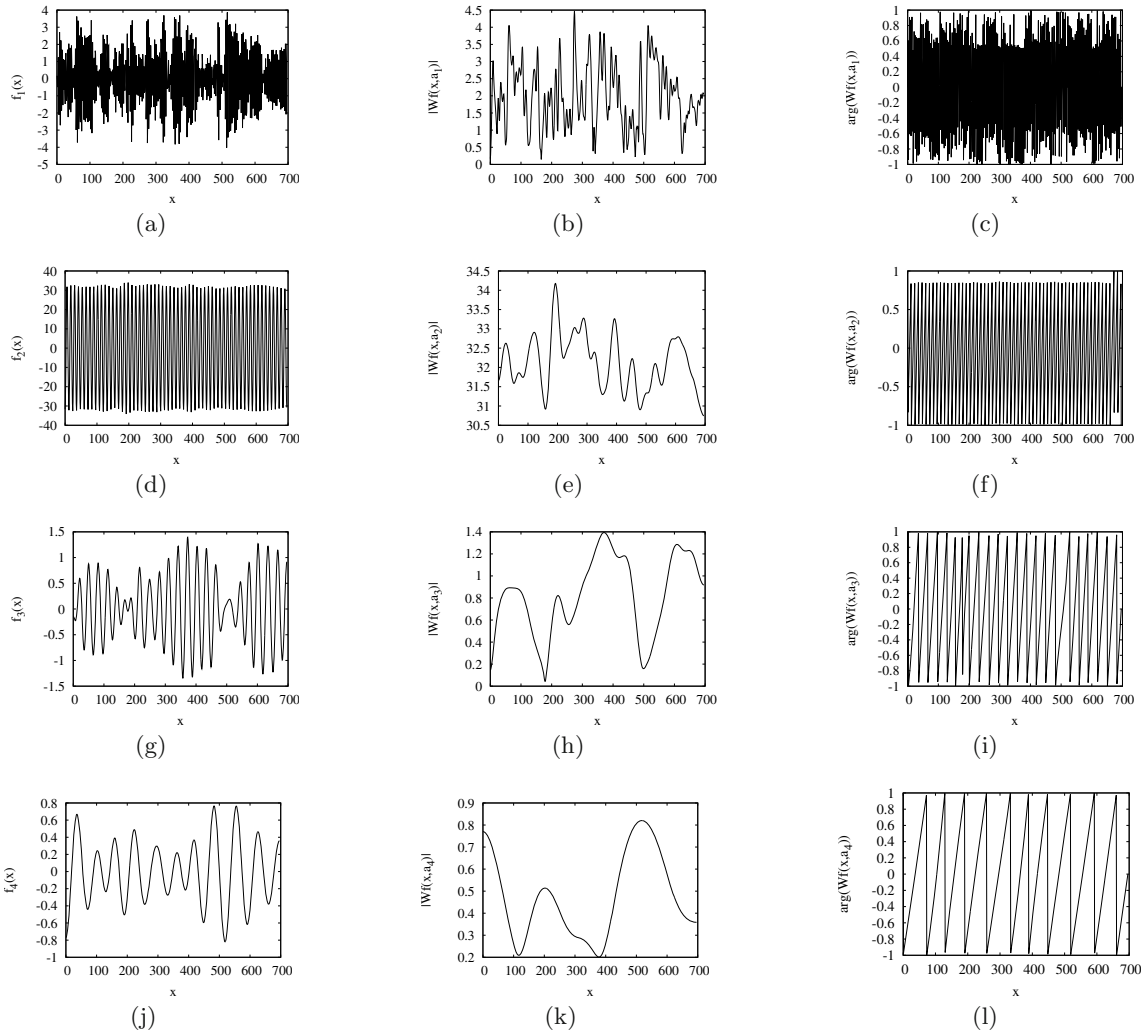

Fig. 14. The wavelet decomposition of the near-surface air temperature time series from Verhojansk: the first (a), the second (d), the third (g) and the fourth (j) component, as well as the modulus of the first (b), the second (e), the third (h) and the fourth (k) component and the phase of the first (c), the second (f), the third (i) and the fourth (l) component.

and 68 months respectively (see Fig. 13). The amplitude associated to the cycles are 1.98, 32.14, 0.83 and 0.48 degrees respectively.

The decomposition proposed here therefore leads to four modes f_1, f_2, f_3 and f_4 (see Figs. 14a, 14d, 14g and 14j). The correlation between the temperature data and $f_1+f_2+f_3+f_4$ is larger than 0.995, while the RMSE is smaller than 2.13.

Since it is related to the highest frequency, the first component (corresponding to 4 months) can be associated to a background noise, while the second (associated to 12 months) is obviously the annual cycle. The presence of the two later components (associated to 30 and 68 months respectively) is more astonishing. Such periods have already been detected in climatological data (see e.g. [21,22]). Moreover, these periods are observed in the climatic anomaly associated to Verhojansk with the Fourier spectrum. Such a signal is computed by subtracting the monthly mean to the near-surface air temperature data, in order to remove the annual cycle: if $x_{j,k}$ is the temperature data measured the j-th month of the year k, one computes $m_j = M(x_{j,.})$, where M denotes the mean (over the years), to obtain the climatic anomaly time series, $x'_{j,k} = x_{j,k} - m_j$. The Fourier spectrum of the climatic anomaly time series clearly displays maxima associated to periods of 30 (the spectrum displays two maxima at $1/\nu = 29.4$ and $1/\nu = 32$) and 68 (the spectrum displays a maximum at $1/\nu = 63.5$) months, as shown in Figure 15.

4.2 Discussion

As expected, since the annual cycle is of very high amplitude; f_2 is highly correlated to f (the correlation between these two signals is equal to 0.99 ± 0.001), but the RMSE between f and f_2 is larger than 2.69, while the RMSE between f and $f_1+f_2+f_3+f_4$ is smaller than 2.13. Moreover, the RMSE between f and f_2 is smaller than the RMSE between f and the monthly mean (defined above), which

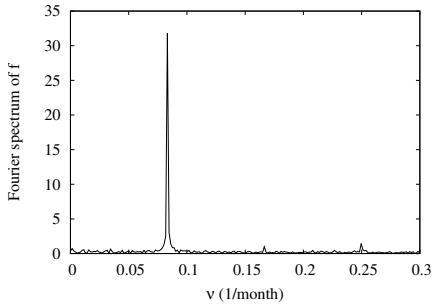

(a)

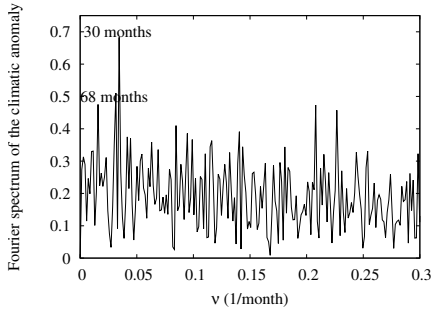

(b)

Fig. 15. The Fourier spectra of the near-surface air temperature time series of Verhojansk (a) and the climatic anomaly time series obtained from these data (b).

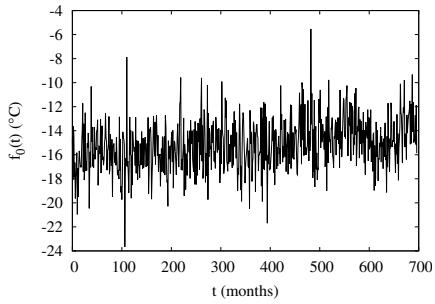

Fig. 16. The component f_0 of the near-surface air temperature time series of Verhojansk.

is equal to 2.97. However, f_2 is very close to the monthly mean, since the correlation between these two signals is larger than 0.997, while the RMSE is lower than 1.7.

When considering such a signal, it is also interesting to look at the "remaining component" $f - f_1 - f_2 - f_3 - f_4$ (see Fig. 16), which can be considered as the part of the signal that can not be explained in terms of oscillatory components. One can suspect a linear trend during the last seven years (although further investigation should be carried out). The mean and the standard deviation of f_0 are equal to -15.16 and 2.13 respectively. Let us also remark that performing a new wavelet-based decomposition on f_0 does not lead to significant periods (data not shown). If one fits f_0 with the linear model $ax + b$, one gets, using the LM algorithm (see [23]), $a = 34 \times 10^{-4} \pm 38 \times 10^{-5}$ and $b = -16.21 \pm 0.16$, which could mean that the "mean temperature" has increased about 2.4 degrees in Verhojansk during the last fifty years.

4.3 Conclusion

As a conclusion, one can decompose the near-surface air temperature time series of Verhojansk into four components associated to the periods of 4, 12, 30 and 68 months respectively. One can estimate the contribution of each component to the total temperature variation: the mean amplitudes of f_1, f_2, f_3 and f_4 are approximatively equal to 1.98, 32.14, 0.83 and 0.48 degrees respectively. Other weather stations would lead to similar results, although a period of 43 months is sometimes observed instead of the period of 30 months (see [16]). Moreover, it has been shown that the cycle corresponding to 30 months is statistically significant (see [24,25]); using the method described in [25], one gets that this cycle in Verhojansk is significant with a α-level smaller than 5%. Finally, one can estimate, looking at f_0, that the mean temperature in Verhojansk has increased about 2.4 degrees in fifty years.

The author would like to thank P. Flandrin for helpful comments and suggestions on a prior draft and M. Mudelsee for his suggestions that have improved the paper.

References

1. M. Mudelsee, *Climate Time Series Analysis: Classical Statistical and Bootstrap Methods* (Springer, Dordrecht, 2010)
2. M.B. Priestley, *Spectral Analysis and Time Series* (Academic Press, London, 1981), Vols. I and II
3. E.C. Titchmarsh, *Introduction to the Theory of Fourier Integrals* (Oxford University Press, 1948)
4. P. Goupillaud, A. Grossman, J. Morlet, Geoexploration **23**, 85 (1984)
5. R. Kronland-Martinet, J. Morlet, A. Grossmann, Int. J. Pattern Recogn. Artific. Intellig. **1**, 273 (1987)
6. N.E. Huang et al., Proc. Roy. Soc. London A **454**, 903 (1998)
7. G. Rilling, P. Flandrin, IEEE transactions on signal processing **56**, 85 (2008)
8. I. Daubechies, *Ten Lectures on Wavelets* (SIAM, Philadelphie, 1992)
9. S. Mallat, *A Wavelet Tour of Signal Processing* (Academic Press, New-York, 1999)
10. B. Torresani, *Analyse Continue par Ondelettes* (CNRS Éditions, Paris, 1995)
11. E. Freysz, B. Pouligny, F. Argoul, A. Arneodo, Phys. Rev. Lett. **64**, 745 (1990)
12. A. Arneodo, B. Audit, N. Decoster, J.-F. Muzy, C. Vaillant, *The Science of Disaster*, edited by A. Bunde, H.J. Schellnhuber (Springer, Berlin, 2002), pp. 27–102
13. *Wavelets and their Applications*, edited by M.B. Ruskai, G. Beylkin, R. Coifman, I. Daubechies, S. Mallat, Y. Meyer, L. Raphael (Jones and Bartlett, Boston, 1992)
14. M.B. Priestley, J. Time Ser. Anal. **17**, 85 (1996)

15. S. Nicolay, *Analyse de séquences ADN par la transformée en ondelettes*, Ph.D. thesis, University of Liège, 2009
16. S. Nicolay, G. Mabille, X. Fettweis, M. Erpicum, Clim. Dyn. **33**, 1117 (2006)
17. S.L. Hahn, *Hilbert transforms in signal processing* (Artech House, Boston, 1996)
18. D.B. Percival, A.T. Walden, *Spectral analysis for physical applications* (Cambridge University Press, Cambridge, 1993)
19. J. Hansen, R. Ruedy, J. Glascoe, M. Sato, J. Geophys. Res. **104**, 30997 (1999)
20. W. Rudloff, *World-climates* (Wissenschaftliche Verlagsgesellschaft mbH, 1981)
21. I. Matyasovszky, Theor. Appl. Climatol. **101**, 281 (2010)
22. M. Paluš, D. Novotná, Nonlinear Proc. Geophys., **13**, 287 (2006)
23. K. Levenberg, Quart. Appl. Math. **2**, 164 (1944)
24. G. Mabille, S. Nicolay, Eur. Phys. J. Special Topics **174**, 135 (2009)
25. S. Nicolay, G. Mabille, X. Fettweis, M. Erpicum, Nonlinear Processes Geophysics **17**, 269 (2010)